MODERN NONLINEAR OPTICS
Part 2

Edited by

MYRON EVANS
Department of Physics
The University of North Carolina
Charlotte, North Carolina

STANISŁAW KIELICH
Nonlinear Optics Division
Institute of Physics
Adam Mickiewicz University
Poznań, Poland

ADVANCES IN CHEMICAL PHYSICS
VOLUME LXXXV

Series Editors

ILYA PRIGOGINE
University of Brussels
Brussels, Belgium
and
University of Texas
Austin, Texas

STUART A. RICE
Department of Chemistry
and
The James Frank Institute
University of Chicago
Chicago, Illinois

AN INTERSCIENCE® PUBLICATION
JOHN WILEY & SONS, INC.
NEW YORK • CHICHESTER • BRISBANE • TORONTO • SINGAPORE

MODERN NONLINEAR OPTICS
Part 2

ADVANCES IN CHEMICAL PHYSICS

VOLUME LXXXV

MODERN NONLINEAR OPTICS
Part 2

Edited by

MYRON EVANS
Department of Physics
The University of North Carolina
Charlotte, North Carolina

STANISŁAW KIELICH
Nonlinear Optics Division
Institute of Physics
Adam Mickiewicz University
Poznań, Poland

ADVANCES IN CHEMICAL PHYSICS
VOLUME LXXXV

Series Editors

ILYA PRIGOGINE
University of Brussels
Brussels, Belgium
and
University of Texas
Austin, Texas

STUART A. RICE
Department of Chemistry
and
The James Frank Institute
University of Chicago
Chicago, Illinois

AN INTERSCIENCE® PUBLICATION
JOHN WILEY & SONS, INC.
NEW YORK • CHICHESTER • BRISBANE • TORONTO • SINGAPORE

This text is printed on acid-free paper.

An Interscience® Publication

Library of Congress Catalog Number: 58-9935

ISBN 0-471-57546-1

Printed in the United States of America

10 9 8 7 6 5 4 3 2

CONTRIBUTORS TO VOLUME LXXXV
Part 2

DAVID L. ANDREWS, School of Chemical Sciences, University of East Anglia, Norwich, England

H. J. CAULFIELD, Department of Physics, Alabama A&M University, Normal, Alabama

W. T. COFFEY, School of Engineering, Department of Microelectronics & Electrical Engineering, Trinity College, Ireland

MYRON W. EVANS, Department of Physics, University of North Carolina, Charlotte, North Carolina

AHMED A. HASANEIN, Department of Chemistry, Faculty of Science, Alexandria University, Alexandria, Egypt

H. JAGANNATH, Department of Physics, Alabama A&M University, Normal, Alabama

YU. P. KALMYKOV, Institute of Radio Engineering and Electronics, Russian Academy of Sciences, Fryazino, Russia

AKHLESH LAKHTAKIA, Department of Engineering Science and Mechanics, The Pennsylvania State University, University Park, Pennsylvania

E. S. MASSAWE, School of Engineering, Department of Microelectronics & Electrical Engineering, Trinity College, Dublin, Ireland

A. S. PARKINS, Department of Physics, University of Waikato, Hamilton, New Zealand

G. E. STEDMAN, Department of Physics, University of Canterbury, New Zealand

JEFFREY HUW WILLIAMS, Institut Max von Laue-Paul Langevin, Grenoble, France

INTRODUCTION

Few of us can any longer keep up with the flood of scientific literature, even in specialized subfields. Any attempt to do more and be broadly educated with respect to a large domain of science has the appearance of tilting at windmills. Yet the synthesis of ideas drawn from different subjects into new, powerful, general concepts is as valuable as ever, and the desire to remain educated persists in all scientists. This series, *Advances in Chemical Physics*, is devoted to helping the reader obtain general information about a wide variety of topics in chemical physics, a field that we interpret very broadly. Our intent is to have experts present comprehensive analyses of subjects of interest and to encourage the expression of individual points of view. We hope that this approach to the presentation of an overview of a subject will both stimulate new research and serve as a personalized learning text for beginners in a field.

ILYA PRIGOGINE
STUART A. RICE

PREFACE

Statistical molecular theories of electric, magnetic, and optical saturation phenomena developed by S. Kielich and Piekara in several papers in the late 1950s and 1960s clearly foreshadowed the developments of the next thirty years. In these volumes, we as guest editors have been honored by a positive response to our invitations from many of the most eminent contemporaries in the field of nonlinear optics. We have tried to give a comprehensive cross section of the state of the art of this subject. Volume 85 (Part 1) contains fourteen review articles by the Poznań School and associated laboratories, and volume 85 (Part 2 and Part 3) contain a selection of reviews contributed from many of the leading laboratories around the world. We thank the editors, Ilya Prigogine and Stuart A. Rice, for the opportunity to produce this topical issue.

The frequency with which the work of the Poznań School has been cited in these volumes is significant, especially considering the overwhelming societal difficulties that have faced Prof. Dr. Kielich and his School over the last forty years. Their work is notable for its unfailing rigor and accuracy of development and presentation, its accessibility to experimental testing, the systemic thoroughness of the subject matter, and the fact that it never seems to lag behind developments in the field. This achievement is all the more remarkable in the face of journal shortages and the lack of facilities that would be taken for granted in more fortunate centers of learning.

We hope that readers will agree that the contributors to these volumes have responded with readable and useful review material with which the state of nonlinear optics can be measured in the early 1990s. We believe that many of these articles have been prepared to an excellent standard. Nonlinear optics today is unrecognizably different from the same subject in the 1950s, when lasers were unheard of and linear physics ruled. In these two volumes we have been able to cover only a fraction of the enormous contemporary output in this field, and many of the best laboratories are not represented.

We hope that this topical issue will be seen as a sign of the ability of scientists all over the world to work together, despite the frailties of human society as a whole. In this respect special mention is due to Professor Mansel Davies of Criccieth in Wales, who was among the first in the West to recognize the significance of the output of the Poznań School.

MYRON W. EVANS

Charlotte, North Carolina
October 1993

CONTENTS

HOLOGRAPHY AND DOUBLE PHASE CONJUGATION

H. JAGANNATH AND H. J. CAULFIELD

Department of Physics, Alabama A & M University, Normal, AL

CONTENTS

Modern Nonlinear Optics, Part 2, Edited by Myron Evans and Stanisław Kielich. Advances in Chemical Physics Series, Vol. LXXXV.
ISBN 0-471-57546-1

I. INTRODUCTION

Two- and four-wave mixing processes in nonlinear optics have proved to be extremely useful. Several applications in optical image processing, optical communications, real-time holography, and opto-electronic neural networks have been developed in recent years. Both processes are accurately and appropriately described in terms of ordinary holography occurring in real time. The spatial or temporal interference between coherent beams spatially modulates the characteristics of the recording medium, storing information. This information can be retrieved simultaneously or later with another coherent beam. Wave mixing between mutually incoherent beams is a new phenomenon which occurs in the same materials. Double phase conjugation is one such mutually incoherent beam-coupling process, which also produces accurate three-dimensional images. Though there are some similarities between real-time holography and double phase conjugation, we will show that there are distinct differences between the two processes, requiring a new holographic interpretation of double phase conjugation. The advantage of this interpretation is that double phase conjugation can be viewed as a more general form of holography—holography with mutually incoherent sources.

This chapter is devoted to double phase-conjugate mirror (DPCM). Real-time holography and all multiwave mixing processes including mutually incoherent beam coupling (MIBC) are dynamic self-diffraction processes. We present a comprehensive review of holography (Section II), volume holography and dynamic self-diffraction (Section III), two- and four-wave mixing (Sections IV–VI), and mutually incoherent beam coupling (Section VII) to establish a link between holography and double phase conjugation. Emphasis is placed mostly on the studies with photorefractive materials, because they are the materials of choice for MIBC/DPCM and real-time holography. The double phase-conjugate mirror is reviewed in Section VIII. The holographic interpretation of the two- and four-wave mixing processes and the physical mechanism responsible for MIBC lead us to believe that DPCM is a new type of holography in which the primary holograms interact to create another hologram. This "second-order" holography is explored in Section IX. Finally, the relaxed stability and coherence requirements of the incident beams lead to new applications in optical imaging and optical communications, some of which are presented in Section X. Due to the limited scope of this chapter, the interested reader is referred to other chapters in the book and to the following for additional information: photorefractive materials and their applications,[1-3, 7] volume holography,[4-6, 23] two-wave mixing,[17] degenerate four-wave mixing and phase conjugation,[3, 53] and photorefractive oscillators.[17, 40, 68]

II. HOLOGRAPHY

Holography is an optical process by which storage and retrieval of optical wavefronts is possible. Spatial information about the object is contained in the time evolution of the two-dimensional wavefronts emanating from the object. Complete information about the phase and amplitude of the wavefronts is needed to reconstruct the original object. Since recording materials do not respond to the phase directly, interferometric techniques are used to record the phase information. This places severe restrictions on the illuminating beams. For good contrast fringes and hence good efficiency, the illuminating source must have good coherence properties. High mechanical stability of the source and the object is required because of the time requirements of recording. The availability of monochromatic coherent laser sources has made possible the three-dimensional imaging of objects and has led to a large number of industrial applications. Holographic processing involves two steps: (1) recording and (2) reconstructing of the object wavefront. We review each briefly.

A. Holographic Recording

In the recording process, mutually coherent object and reference wavefronts are brought together to interfere (Fig. 1). A recording medium, such as a photographic plate, placed in the overlap region of the two wavefronts records the interference pattern.

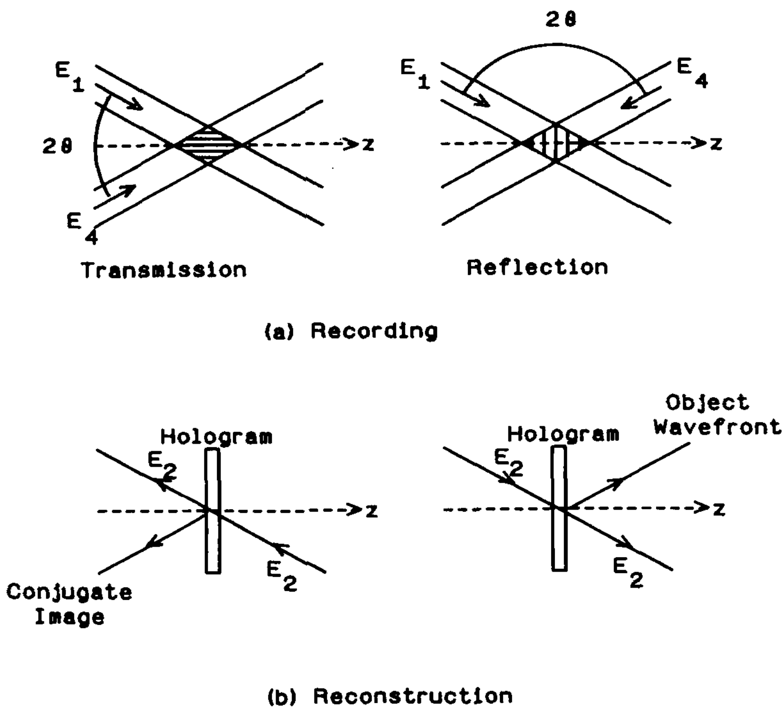

Figure 1. Holographic recording and wavefront reconstruction. E_1 and E_4 are the object and reference beams, respectively; E_2 is the reconstructing beam.

Assuming that the two beams are plane waves with parallel polarizations, the electric field of the object wavefront can be written as

$$E_1(\mathbf{r}) = A_1 \exp[-i(\omega t - \mathbf{k}_1 \cdot \mathbf{r})] \tag{1}$$

and that of the reference wavefront as

$$E_4(\mathbf{r}) = A_4 \exp[-i(\omega t - \mathbf{k}_4 \cdot \mathbf{r})] \tag{2}$$

The intensity I_T of the light in the overlapping region is given by

$$I_T = |E_1(\mathbf{r}) + E_4(\mathbf{r})|^2 \tag{3}$$

For a recording medium in the xy plane, if the direction of propagation is along the z axis, and 2ϑ is the angle between the wave vectors $\mathbf{k}_1$ and $\mathbf{k}_4$,

$$I_{\mathrm{T}} = A_0^2\left[1 + m\cos\left(\frac{2\pi y}{d}\right)\right] \tag{4}$$

where m is the modulation depth given by

$$m = \frac{2A_0A_{\mathrm{R}}}{A_0^2 + A_{\mathrm{R}}^2} \tag{5}$$

and $d = \lambda/2\sin\vartheta$ is the spacing between the inteference maxima.

The spatial variance in the light intensity corresponding to the total field is recorded in the medium in the form of either an optical density pattern leading to an absorption grating or a phase shift pattern leading to a phase hologram. The transmission $T(y)$ of the electric vector through the absorption grating generated by I_{T} can be expressed as[5]

$$T(y) = T_0 + \beta E_0 m\cos Ky \tag{6}$$

where $K = 2\pi/d$ is the grating vector, T_0 is constant field transmission, E_0 is the exposure, and β is the transfer characteristic of the recording material.

In a phase grating the field transmission is given by[5]

$$T(y) \propto \left\{J_0(\phi_1) + 2\sum\left[J_n(\phi_1)\frac{\cos(nKy)}{\mathrm{i}^n}\right]\right\} \tag{7}$$

where $J_n(\phi_1)$ are the Bessel functions of the phase modulation ϕ_1. $J_0(\phi_1)$ contributes to the constant background, while $J_1(\phi_1)$ contributes to the first-order diffracted intensity in reconstruction.

B. Wavefront Reconstruction

To reconstruct the object wavefront, we illuminate the holographic recording or hologram by a reconstruction beam E_2 (Fig. 1b). The transmitted wave-front field for the case of absorption grating is given by

$$T(y) = E_2\,\mathrm{e}^{-\mathrm{i}\omega t}\left[T_0\,\mathrm{e}^{\mathrm{i}ky} + \tfrac{1}{2}\beta E_0 m\left[\mathrm{e}^{-\mathrm{i}(K-k)y} + \mathrm{e}^{\mathrm{i}(K+k)y}\right]\right] \tag{8}$$

The first term is a plane wave propagating in the direction of the reconstruction beam. The second term corresponds to the primary image beam. The third term corresponds to a beam traveling in the opposite direction to the object beam, and forms the conjugate image. In the case of phase gratings, reconstruction by the illuminating beam leads to the undeviated, object, and conjugate beams.

The diffraction efficiency of the hologram is defined as the ratio of the intensity of the reconstructed wavefront to the intensity of the reconstruction beam. The maximum efficiency of transmission hologram with a single-layer absorption grating is 0.0625, and that of a phase grating is 0.339. A single-layer reflective hologram is a reflection grating that can be blazed to obtain high diffraction efficiency. Reflection holograms with reconstruction efficiencies of 0.85 have been reported.

III. VOLUME HOLOGRAPHY

The efficiency of a hologram can be improved by increasing the thickness of the recording medium. This allows for more diffraction gratings to be written in the recording medium. The hologram with multiple layers of recording is called a "thick" hologram. If d is the thickness and Λ is the grating spacing, then for a thick hologram $d > n\Lambda^2/2\pi\lambda$. For sufficiently thick recording materials, the total beam overlap volume can be used to write a volume hologram. Because of the multiple planes at which light diffraction occurs in a thick hologram during reconstruction process, diffraction at or near the Bragg angle leads to efficient wave-front reconstruction. The higher diffraction orders are quenched by interference. This is true for both transmission and reflection holograms.

A. Thick Gratings and Beam Coupling

In thick gratings, the illuminating beam is strongly depleted as it propagates through the material due to large diffraction efficiency. Within the hologram, two mutually coherent beams are traveling: the incoming reference beam E_1 and the outgoing signal beam E_4 (Fig. 2). As the beams propagate, each beam is diffracted in the direction of the other beam at the grating surfaces. Energy exchange takes place between the beams and the beams are coupled. Kogelnik[6] analyzed these spatially dynamic interaction processes in terms of the coupled wave theory and obtained expressions for diffraction efficiencies for reflection and transmission holograms with absorption and phase gratings.

Wave propagation in the holographic grating is described by the scalar wave equation

$$\nabla^2 E + k^2 E = 0 \tag{9}$$

For small amplitudes of spatial modulations in the refractive index n_1 and

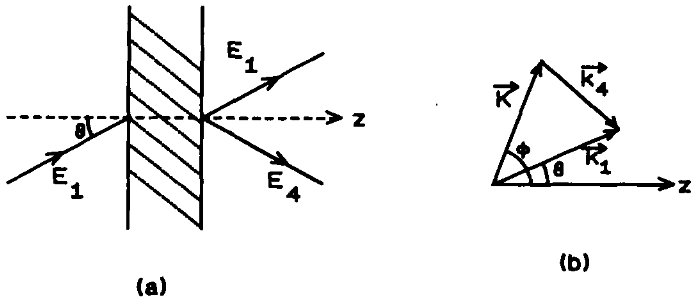

Figure 2. Beam coupling in a volume hologram: (a) geometry of the interacting beams; (b) wave-vector diagram. **K** is the grating vector.

the absorption coefficient α_1, the propagation constant k in the material can be expressed in terms of the dielectric constant ε_0, the average conductivity σ_0, the grating vector **K**, and, the coupling constant κ as

$$k^2 = \beta^2 - 2\mathrm{i}\alpha\beta + 2\kappa\beta(\mathrm{e}^{\mathrm{i}\mathbf{K}\cdot\mathbf{r}} + \mathrm{e}^{-\mathrm{i}\mathbf{K}\cdot\mathbf{r}}) \tag{10}$$

where

$$\beta = \frac{2\pi\varepsilon_0^{1/2}}{\lambda} \qquad \alpha = \frac{\mu c\sigma_0}{2\varepsilon_0^{1/2}} \qquad \kappa = \frac{\pi n_1}{\lambda} - \frac{\mathrm{i}\alpha_1}{2} \tag{11}$$

κ describes the coupling between the reference beam E_1 and signal beam E_4. Amplitudes $A_1(z)$ and $A_4(z)$ vary along the propagation direction as a result of the coupling. The wave vector $\mathbf{k}_4$ is forced by the grating to satisfy the relation $\mathbf{k}_4 = \mathbf{k}_1 - \mathbf{K}$.

If the reference beam is incident at an angle ϑ with respect to the direction of propagation z, and the grating wave vector **K** is slanted at an angle ϕ, the Bragg condition is given by

$$\cos(\phi - \vartheta) = \frac{K}{2\beta} \tag{12}$$

From the scalar wave equation (9), assuming that the $A_1(z)$ and $A_4(z)$ vary slowly, the following set of coupled equations are obtained:

$$c_\mathrm{R}\frac{\mathrm{d}A_1}{\mathrm{d}z} + \alpha A_1 = -\mathrm{i}\kappa A_4 \tag{13}$$

$$c_\mathrm{S}\frac{\mathrm{d}A_4}{\mathrm{d}z} + (\alpha + \mathrm{i}\theta)A_4 = -\mathrm{i}\kappa A_1 \tag{14}$$

where $c_R = \cos\vartheta$, $c_S = \cos\vartheta - K/2\beta$, and θ is the dephasing measure given by

$$\theta = K\cos(\phi - \vartheta) - \frac{K^2\lambda}{4\pi n} \tag{15}$$

The physical picture of the diffraction process is reflected in the coupled equations (13)–(15). As the waves propagate in the material, the amplitudes of the waves change due to coupling to the other waves ($\kappa A_1, \kappa A_4$), to absorption ($\alpha A_1, \alpha A_4$), or to both. For deviation from the Bragg condition, the two beams are forced out of synchronization and the interaction decreases.

A complete analysis of the wave propagation in lossless, lossy, and slanted, transmission, and reflection holograms was given by Kogelnik.[6] The results show that the diffraction efficiencies are less for absorption gratings than for phase gratings. The maximum diffraction efficiencies are 0.037 and 0.072 for lossless, unslanted absorption gratings in transmission and reflection holograms, respectively. The grating slant improves the efficiencies of the lossy absorption gratings, though the maximum efficiencies are still below those of the lossless gratings. The maximum diffraction efficiency for lossless, unslanted phase grating is ~ 1.00 both for transmission and reflection holograms. As in the case of absorption gratings, the efficiency of the lossy phase gratings can be improved by grating slant. All these results have been verified experimentally.

One of the important applications of volume holography is in information storage in holographic memory systems. The diffraction limited storage densities attainable in volume holograms are very high. Several materials, such as photographic emulsions, photochromic glasses, dichromate sensitized gelatin, alkali halide, and electro-optical crystals, have been used in these applications. The condition for the thick holograms, $Q = 2\pi\lambda d/n\Lambda^2 \gg 1$, can be easily met for thickness d of a few micrometers. Of all these recording materials, the electro-optic crystals are of particular interest since the phase grating in these materials is phase shifted from the sinusoidal light interference pattern. The result is a strong coupling of the writing beams during the recording process. This leads to nonreciprocal energy exchange and self-diffraction of the writing beams.

B. Photorefractive Materials

The electro-optic materials in which the refractive indices are changed by light-induced electric fields are called photorefractive materials. A large number of materials have been observed to show photorefraction at moderately low illuminations; $BaTiO_3$, $Bi_{12}SiO_{20}$(BSO), $Bi_{12}GeO_{20}$(BGO), $Bi_{12}TiO_{20}$(BTO), $KNbO_3$, $LiNbO_3$, and $Sr_xBa_{1-x}Nb_2O_6$(SBN). The materials are intrinsically transparent in the visible region. But the presence of impurities permits the generation of photoexcited charges which lead to light-induced fields under nonuniform illumination. The materials are erasable and can be used for read–write applications.

The generation and transportation of charge carriers in electro-optic materials have been investigated by several workers.[7] Two charge transportation mechanisms have been proposed. In the charge hopping model,[8] the charge carriers that are excited from the donor sites in the presence of light, hop to adjacent sites with a probability proportional to the intensity of the light. The drift of the carriers by hopping continues in all directions until the carriers are out of the illuminated areas, resulting in a net electric field. In the band-conduction model[9] (Fig. 3a), the charge carriers are excited from the donor levels to the conduction band. The charges

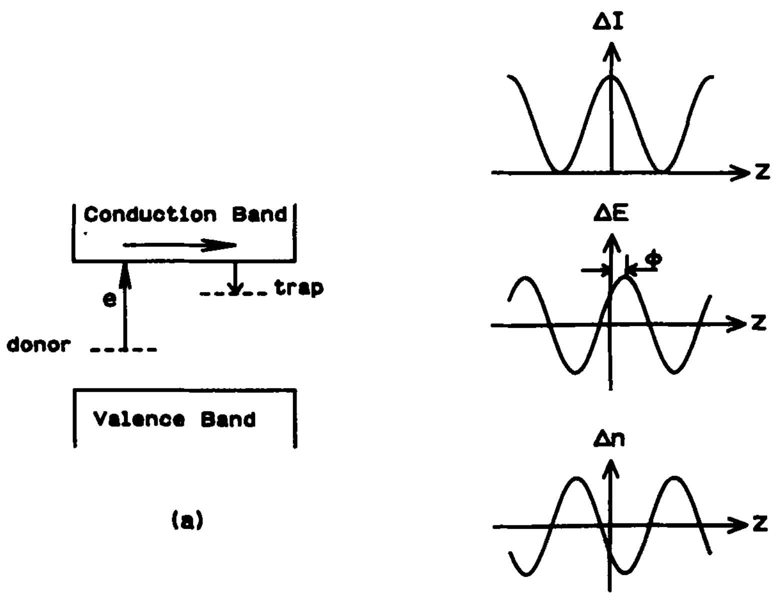

(b)

Figure 3. (a) Energy-level diagram of a photorefractive material in the band conduction model; (b) the spatial distribution of the intensity I, the space-charge field E, and the refractive index n under sinusoidal illumination. Φ is the phase shift between the light-intensity pattern and the space-charge field.

then diffuse or drift in the presence of the external fields and are trapped at the acceptor sites. This charge redistribution leads to the space-charge field. The band-conduction model has been widely accepted because it explains space-charge field formation in a variety of materials in which the transportation lengths vary widely. Both positive and negative charge carriers have been observed to take part in the charge transportation processes. The one-carrier, one-donor model discussed below has been extended to simultaneous electron–hole transportation models.[10]

The equation for generation and transportation of the charge carriers can be written as[11-14]

$$e\frac{\partial N_{\mathrm{D}}^{+}}{\partial t} = \frac{\partial J}{\partial z} \qquad \text{Continuity equation} \tag{16}$$

$$\frac{\partial N_{\mathrm{D}}^{+}}{\partial t} = sIN_{\mathrm{D}} - \gamma_{\mathrm{R}} n N_{\mathrm{D}}^{+} \qquad \text{Rate equation} \tag{17}$$

$$J = e\mu n E_{\mathrm{s}} - k_{\mathrm{B}} T \mu \frac{\partial n}{\partial z} \qquad \text{Equation of motion} \tag{18}$$

$$\frac{\partial E_{\mathrm{S}}}{\partial z} = \frac{e}{\varepsilon_0 \varepsilon_{\mathrm{s}}}\left(N_{\mathrm{A}} - N_{\mathrm{D}}^{+}\right) \qquad \text{Poisson's equation} \tag{19}$$

where n is the electron density, N_{D} is density of donors, N_{A} is the density of acceptors, N_{D}^{+} is the density of ionized donors, J is the current density, E_{S} is the space-charge field, I is the light intensity, β_{e} is the rate of thermal generation, s is the rate of photoionization, γ_{R} is the recombination rate, μ is the mobility, and, ε_{s} is the relative static dielectric constant. In the formulation of the above set of equations, the following assumptions have been made: $n \ll N_{\mathrm{D}}^{+}$; $\beta_{\mathrm{e}} \ll sI$; $N_{\mathrm{D}}^{+} \ll N_{\mathrm{D}}$; spatial variations are only along the direction of propagation z; there is no photovoltaic effect; and ε_{s} is independent of z.

Equations (16)–(19) are nonlinear and have been solved under various approximations for spatially periodic light illumination. In the two cases of short time limit and saturation time limit, the equations have been solved in terms of a Fourier series.[15] Another approach, developed by Kukhtarev et al.,[12, 13] assumes solutions of the form

$$a(z,t) = a_0 + \left[a_1(z,t)\mathrm{e}^{\mathrm{i}Kz} + \text{c.c.}\right]/2 \tag{20}$$

where $a = N_{\mathrm{D}}^{+}$, n, J, and E_{s}, and all higher order terms are dropped. If we assume that the modulations in the parameters are small, the material equations can be reduced to[14]

$$\frac{\partial E_s}{\partial t} + gE_s = hm \tag{21}$$

where

$$\begin{aligned}
&g = (E_q + E_D + iE_0)/E_q D\tau_d, \quad h = (E_0 + iE_D)/D\tau_d, \\
&D = (E_M + E_D + iE_0)/E_M \\
&E_D = KTk_B/e, \quad E_q = eN_A/\varepsilon_0\varepsilon_s K, \quad E_M = \gamma_R N_A/\mu K, \\
&\tau_d = \varepsilon_0\varepsilon_s/e\mu n_0, \quad n_0 = sI_0 N_D/\gamma_R N_A
\end{aligned} \tag{22}$$

and m is the fringe modulation.

The steady-state space-charge field is given by $E_s = hm/g$. The phase shift Φ_g between the light intensity pattern and the space-charge field is given by

$$\tan \Phi_g = \frac{E_0^2 + E_D(E_D + E_q)}{E_0 E_q} \tag{23}$$

In general, if both diffusion and drift fields are present, there are two components of the E_s: one that is in phase with the intensity modulation and another whose phase is $\pi/2$ shifted with respect to the intensity modulation. In barium titanate, the charge migration is due to diffusion only. The space-charge field is $\pi/2$ phase shifted from E_s. BSO and other materials have shifted and unshifted space-charge field components. In the absence of external field, and for a modulation $m = 1$, the steady-state space-charge field can be written as

$$E_s = -i\frac{k_B T}{e}\frac{K}{1 + (K/k_0)^2} \tag{24}$$

where $k_0^2 = (e^2 N_A/k_B T\varepsilon_0\varepsilon_s)$.

The measured parameters of relevance for the photosensitivity of some of the photorefractive materials are given in Table I. GaAs, BSO, and BGO have better response times for the grating formation than other materials. The efficiency of beam coupling is larger for barium titanate and SBN.

The mechanism of hologram formation in photorefractive materials is the following.[16] When the material is illuminated by two beams that

TABLE I
Relevant Optical Parameters of Some Photorefractive Materials

Material	λ (μm)	r (pm/V)	n	$\varepsilon/\varepsilon_0$	α (cm^{-1})	τ (s)	γ (cm^{-1})	Q[a] (pm/Vε_0)
$BaTiO_3$[20]	0.5	$r_{42} = 1640$	$n_e = 2.4$	$\varepsilon_1 = 3600$	1.0	1.3[18]	20[18]	6.3
SBN:75[19]	0.5	$r_{33} = 1400$	—	$\varepsilon_{33} = 3000$	—	0.6[19]	—	5.6
SBN:60[19]	0.5	$r_{33} = 40$	—	$\varepsilon_{33} = 900$	—	0.05[19]	14[19]	6.3
SBN:Ce[20]	0.5	$r_{33} = 235$	$n_e = 2.33$	$\varepsilon_c = 880$	0.7	0.8[20]	14[20]	4.8
BSKNN-2[19]	0.5	$r_{33} = 170$	—	$\varepsilon_{11} = 360$	—	0.6[19]	—	6.0
BSO[20]	0.6	$r_{41} = 5$	$n = 2.54$	$\varepsilon = 56$	0.13	0.015[14]	10[14]	1.5
BGO[7]	0.5	$r_{41} = 3.4$	$n = 2.55$	$\varepsilon = 47$	2.1	0.015[7]	3-5[7]	1.2
BTO[21]	0.6	$r_{41} = 5.2$	$n = 2.25$	$\varepsilon = 47$	—	—	2[21]	1.3
$KNbO_3$[20]	0.6	$r_{42} = 380$	$n = 2.3$	$\varepsilon_3 = 240$	3.8	0.1[7]	1-5[7]	19.3
$LiNbO_3$[20]	0.6	$r_{33} = 31$	$n_e = 2.2$	$\varepsilon_3 = 32$	0.1	$\sim 10^2$	5[7]	10.3
GaAs[20]	1.1	$r_{12} = 1.4$	$n_e = 3.4$	$\varepsilon = 123$	1.2	8×10^{-5}	0.4[22]	4.7

[a] $Q = n^3 r/\varepsilon$ is defined as the figure-of-merit of a photorefractive material.

produce sinusoidally modulated light intensity pattern, the donors in the regions of bright illumination are excited (Fig. 3b). The excited charge carriers migrate to regions of dark illumination by diffusion or by drift and are retrapped. There is a charge redistribution and a space-charge field is set up. This field modulates the refractive index of the material by Δn through Pockels effect:

$$\Delta n = r_{\text{eff}} n_0^3 |E_s| \tag{25}$$

and a phase grating is formed. The index modulation can be erased by illuminating the material uniformly. Methods have been developed to fix the holograms permanently.

C. Dynamic Self-diffraction

The volume nature of the hologram that is written in photorefractive materials leads to interaction between the writing beams. Writing and reading of the hologram occur simultaneously. The refractive index modulation induced by the incident beams affect the intensity and phase of the incident beams, which, in turn, modify the index grating. Self-diffraction of the writing beams causes a continuous recording of a new grating which is nonuniform through the thickness of the material. In addition, the gratings may be phase shifted with respect to the light-intensity pattern and slanted or even bent. The dynamic gratings are considerably different from the static gratings.

Dynamic self-diffraction in highly nonlinear media has been of interest for many years.[23] The phenomena of self-focusing, self-defocusing, and other self-action effects have been investigated in many transparent media with cubic and higher order nonlinearities. Strong optical fields incident on the medium bring about local or nonlocal, instantaneous or inertial responses in the medium. The light-induced nonlinearity $\Delta\varepsilon$, in general, can be written as[23]

$$\frac{\partial}{\partial t}(\Delta\varepsilon) = D\frac{\partial^2}{\partial t^2}(\Delta\varepsilon) - v\frac{\partial}{\partial z}(\Delta\varepsilon) - \frac{\Delta\varepsilon}{\tau_\varepsilon} + \beta I + \gamma F\left(\frac{\partial}{\partial z}, \int I\,\mathrm{d}z\right) \quad (26)$$

where the first two terms on the right side describe diffusion and drift components of pump flux along the z axis. These components are responsible for the variation in the number of current carriers or excitons in semiconductors or ferroelectrics, or the fluxes of heat and liquids, if $\Delta\varepsilon$ is proportional to the temperature. The third term describes the relaxation of the excitations. The fourth term corresponds to the local response of the medium determined by the polarizability, and the last term corresponds to the nonlocal response of the medium to the incident radiation. The change in the permittivity $\Delta\varepsilon$ gives rise to complex grating formation. The interaction between the medium and the incident beams are described by time-dependent Maxwell's equations. The theoretical and experimental work on these dynamic interactions was reviewed by Vinetskii et al.[23] We summarize some of the results below.

In static unshifted gratings, the diffraction of two coherent beams is always accompanied by a change in their intensities, except for beams of equal intensity. However, in dynamic gratings, two coherent beams writing unshifted gratings do not take part in energy transfer for any ratio of the intensities. The absence of energy transfer is due to the fact that in the interaction between the gratings and the beams, the gratings adjust in such a way that the energy transfer in the two beams is the same and is mutually compensated for any intensity. The dynamic self-diffraction is always accompanied by energy exchange between the beams if the material response is nonlocal and the dynamic gratings are phase shifted from the light-intensity pattern.

Self-diffraction and transient energy exchange have been observed in materials having noninstantaneous (inertial) local response. The energy redistribution between the beams occurs in time intervals compared with the relaxation time of the light-induced refractive index change. Such energy transfer has been observed in electro-optical crystals in which drift mechanism is operative, and in absorbing liquids in which thermal gratings are formed by the writing beams. An artificial phase mismatch may be created between the index grating and the interference field in local response media if the grating relaxation time is large. The detection medium may be spatially displaced during the writing process to create mismatch. The moving medium method has been used to write dynamic holograms in absorbing media such as liquids and in transparent Kerr media.[17] Beam coupling and energy transfer have also been observed in nondegenerate two-wave mixing processes and in nondegenerate nonlinear processes of SRS and SBS. The universal method of achieving dynamic holography in nonlinear media with instantaneous local response is multiwave mixing. These processes are discussed in later sections.

IV. TWO-BEAM COUPLING IN PHOTOREFRACTIVE MATERIALS

As we saw in Section III, beam coupling in photorefractive materials is a dynamic process in which the incident beam and the material interact with each other. The beam coupling processes are described by Maxwell's equations. The material equations are obtained from the charge carrier generation and transportation relations modeled by Kukhtarev for a single-carrier and single-donor/trap system. The temporal and spatial response of the material is described by the solution to the set of equations. Since the equations are nonlinear, analytical solutions have been obtained for steady-state conditions and under undepleted pump approximation for transient conditions. Numerical methods have been used for obtaining exact solutions to the set of equations.

A. Steady-State Analysis[17]

For two waves E_1 and E_2 propagating in the crystal (Fig. 4), the spatial intensity distribution is given by

$$I = |A_1|^2 + |A_2|^2 + A_1^* A_2 \, e^{-\mathbf{K}\cdot\mathbf{r}} + A_1 A_2^* \, e^{i\mathbf{K}\cdot\mathbf{r}} \tag{27}$$

The space-charge field-induced index modulation can be written as

$$n = n_0 + \frac{n_1}{2I_0} e^{i\Phi} A_1^* A_2 \, e^{-i\mathbf{K}\cdot\mathbf{r}} + \text{c.c.} \tag{28}$$

where $I_0 = |A_1|^2 + |A_2|^2$ is the total intensity, and Φ is the phase shift of the index grating with respect to the interference pattern. The refractive index change n_1 is given by Eq. (25).

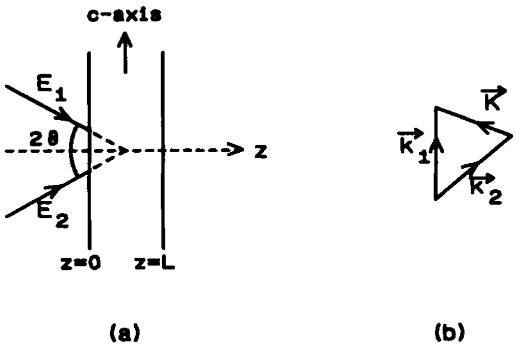

Figure 4. Two-beam coupling in photorefractive materials: (a) beam-interaction geometry; (b) wave-vector diagram.

Wave propagation is described by the scalar wave equation (9). Under SVEA, and from Eq. (28), we obtain the following coupled wave equations for $I_1 = |A_1 \exp(-i\psi_1)|^2$ and $I_2 = |A_2 \exp(-i\psi_2)|^2$:

$$dI_1/dz = -\gamma I - \alpha I_1 \quad (29)$$

$$dI_2/dz = \gamma I - \alpha I_2 \quad (30)$$

$$d\psi_1/dz = \beta I/I_1 \quad (31)$$

$$d\psi_2/dz = \beta I/I_2 \quad (32)$$

where

$$I = \frac{I_1 I_2}{I_1 + I_2} \qquad \gamma = \frac{2\pi n_1}{\lambda \cos(\vartheta/2)} \sin \Phi \qquad \beta = \frac{\pi n_1}{\lambda \cos(\vartheta/2)} \cos \Phi \quad (33)$$

The solutions for Eqs. (29) and (30) are

$$I_1(z) = I_1(0) \frac{1 + m^{-1}}{1 + m^{-1} e^{\gamma z}} e^{-\alpha z} \quad (34)$$

$$I_2(z) = I_2(0) \frac{1 + m}{1 + m\, e^{-\gamma z}} e^{-\alpha z} \quad (35)$$

where $m = I_1(0)/I_2(0)$ is the beam intensity ratio.

The energy exchange between the coupling beams depends on γ. The sign of γ is determined by the orientation of the c axis. If γ is positive and large enough to overcome the absorption, beam 2 is amplified. For sufficiently strong coupling, beam 1 is completely depleted. If γ is negative, the direction of energy transfer process is reversed. As a result, beam 1 is attenuated. The phase shift between the beams $\psi(z)$ is

$$\psi(z) = \psi_2(z) - \psi_1(z) = \psi(0) + \frac{\beta}{\gamma} \ln\left[\frac{e^{\gamma z}(1+m)^2}{(m+e^{\gamma z})^2}\right] \tag{36}$$

The beam coupling gain Γ is

$$\Gamma = \frac{I_2(L)}{I_2(0)} = \frac{1+m}{1+m\,e^{-\gamma L}}\,e^{-\alpha L} \tag{37}$$

For contradirectional beam coupling, the signs of the right-hand-side expressions for I_2 and ψ_2 (Eqs. (30) and (32)) are reversed. The transmittance of the two beams are similar to Eqs. (34) and (35).

B. Transient Analysis

The temporal behavior of the two interacting beams in the transient two-wave mixing (2WM) process depends on the dynamics of the optical fields as well as the dynamics of the nonlinear material in a self-consistent manner. The time-dependent material equation is given by Eq. (21). For small beam interaction lengths, such as occur in many practical situations, we can treat the optical fields as adiabatically following the space-charge field. Under these assumptions, the equations for the optical fields are Eqs. (29) and (30).

The coupled equations have been solved analytically for the case of undepleted pump approximation by several methods in which the boundary conditions are applied in the frequency domain[24-26] as well as in spatial coordinates,[27,28] and by numerical methods for exact solutions.[29-31] The analytical results predict oscillations in the signal beam intensities in the transient regime, which has been experimentally observed.[27] The buildup and decay of the signal beam are complex functions of time even in the case of undepleted pump beams. For positive γL, the decay rate decreases with increasing γL. At high amplification, the signal energy is drawn mostly from the pump beam which is scattered by the grating. The grating strength is not altered at the moment the input signal is cut off, and the output drops off slowly. For negative γL, the steady signal is attenuated by the destructive interference between the signal and the pump beam that is scattered in the direction of the pump beam. After the input signal is turned off, the phase of the signal in the interaction zone reverses. The new signal generates a new grating of opposite phase